Spectrally efficient polarization multiplexed direct-detection OFDM system without frequency gap

Chia-Chien Wei,[1] Wei-Siang Zeng,[2] and Chun-Ting Lin[2,*]

[1]*Department of Photonics, National Sun Yat-sen University, Kaohsiung 804, Taiwan*
[2]*Institute of Photonic System, National Chiao Tung University, Tainan 711, Taiwan*
**jinting@mail.nctu.edu.tw*

Abstract: We experimentally demonstrate a spectrally efficient direct-detection orthogonal frequency-division multiplexing (DD-OFDM) system. In addition to polarization-division multiplexing, removing the frequency gap further improves the spectral efficiency of the OFDM system. The frequency gap between a reference carrier and OFDM subcarriers avoids subcarrier-to-subcarrier beating interference (SSBI) in traditional DD-OFDM systems. Without dynamic polarization control, the resulting interference after square-law direct detection in the proposed gap-less system is polarization-dependent and composed of linear inter-carrier interference (ICI) and nonlinear SSBI. Thus, this work proposes an iterative multiple-input multiple-output detection scheme to remove the mixed polarization-dependent interference. Compared to the previous scheme, which only removes ICI, the proposed scheme can further eliminate SSBI to achieve the improvement of ~ 7 dB in signal-to-noise ratio. Without the need for polarization control, we successfully utilize 7-GHz bandwidth to transmit a 39.5-Gbps polarization multiplexed OFDM signal over 100 km.

OCIS codes: (060.4080) Modulation; (060.4230) Multiplexing; (060.4510) Optical communications.

References and links

1. S. L. Jansen, A. Al Amin, H. Takahashi, I. Morita, and H. Tanaka, "132.2-Gb/s PDM-8QAM-OFDM transmission at 4-b/s/Hz spectral efficiency," IEEE Photon. Technol. Lett. **21**, 802–804 (2009).
2. N. Cvijetic, "OFDM for next-generation optical access networks," J. Lightwave Technol. **30**, 384–398 (2012).
3. H. Takahashi, A. Al Amin, S. L. Jansen, I. Morita, and H. Tanaka, "Highly spectrally efficient DWDM transmission at 7.0 b/s/Hz using 8×65.1-Gb/s coherent PDM-OFDM," J. Lightwave Technol. **28**, 406–414 (2010).
4. D.-Z. Hsu, C.-C. Wei, H.-Y. Chen, W.-Y. Li, and J. Chen, "Cost-effective 33-Gbps intensity modulation direct detection multi-band OFDM LR-PON system employing a 10-GHz-based transceiver," Opt. Express **19**, 17546–17556 (2011).
5. C.-C. Wei, "Small-signal analysis of OOFDM signal transmission with directly modulated laser and direct detection," Opt. Lett. **36**, 151–153 (2011).
6. B. J. C. Schmidt, A. J. Lowery, and J. Armstrong, "Experimental demonstrations of electronic dispersion compensation for long-haul transmission using direct-detection optical OFDM," J. Lightwave Technol. **26**, 196–203 (2008).
7. W.-R. Peng, B. Zhang, K.-M. Feng, X. Wu, A. E. Willner, and S. Chi, "Spectrally efficient direct-detected OFDM transmission incorporating a tunable frequency gap and an iterative detection techniques," J. Lightwave Technol. **27**, 5723–5735 (2009).
8. B. J. Schmidt, Z. Zan, L. B. Du, and A. J. Lowery, "120 Gbit/s over 500-km using single-band polarization-multiplexed self-coherent optical OFDM," J. Lightwave Technol. **28**, 328–335 (2010).

#253910 Received 13 Nov 2015; revised 8 Jan 2016; accepted 12 Jan 2016; published 22 Jan 2016

9. W.-R. Peng, K.-M. Feng, and A. E. Willner, "Direct-Detected Polarization Division Multiplexed OFDM Systems with Self-Polarization Diversity," in IEEE Lasers and Electro-Optics Society (LEOS) 2008, paper MH3.
10. A. A. Amin, H. Takahashi, I. Morita, and H. Tanaka, "100-Gb/s direct-detection OFDM transmission on independent polarization tributaries," IEEE Photon. Technol. Lett. **22**, 468–470 (2010).
11. C.-C. Wei, C.-T. Lin, and C.-Y. Wang, "PMD tolerant direct-detection polarization division multiplexed OFDM systems with MIMO processing," Opt. Express **20**, 7316–7322 (2012).
12. C.-Y. Wang, C.-C. Wei, C.-T. Lin, and S. Chi, "Direct-detection polarization division multiplexed orthogonal frequency-division multiplexing transmission systems without polarization tracking," Opt. Lett. **37**, 5070–5072 (2012).
13. T. N. Duong, N. Genay, M. Ouzzif, J. Le Masson, B. Charbonnier, P. Chanclou, and J. C. Simon, "Adaptive loading algorithm implemented in AMOOFDM for NG-PON system integrating cost-effective and low-bandwidth optical devices," IEEE Photon. Technol. Lett. **21**, 790792 (2009).
14. C.-C. Wei, C.-T. Lin, C.-Y. Wang, and F.-M. Wu, "A novel polarization division multiplexed OFDM system with a direct-detection BLAST-aided receiver," in Proceedings of OFC 2013, JTh2A.49.

1. Introduction

Thanks to the recent advancement of digital signal processing (DSP), orthogonal frequency-division multiplexing (OFDM) has been emerged as a potential format for fiber communication systems [1–4]. Combined with quadrature amplitude modulation (QAM), OFDM can achieve high spectral efficiency (SE). In contrast to coherent detection [1], the direct-detection (DD) scheme is an alternative approach to cost-effectively detect optical OFDM signals. As using the DD scheme, single-sideband (SSB) OFDM generated by a Mach-Zehnder modulator (MZM) is free from dispersion-induced power fading [5]. However, the DD scheme requires a reference optical carrier sent along with an OFDM signal, and an SSB DD-OFDM signal requires an extra frequency gap between a reference carrier and OFDM subcarriers. The frequency gap, of which the width is identical to signal bandwidth, can prevent the received signal from being interfered by nonlinear interference; i.e., subcarrier-to-subcarrier beating interference (SSBI) [6]. To reduce the gap for seeking higher SE, an iterative detection scheme was used to eliminate the SSBI [7]. Another means to improve SE is the polarization-division multiplexing (PDM) technique, and a polarization-diverse receiver can detect PDM signals [1]. Nonetheless, a DD-PDM-OFDM signal requires the reference carrier to be equally separated into two detectors of a polarization-diverse receiver [8]; thus, impractical dynamic polarization control is needed to adjust the state of polarization (SoP) of the co-propagated reference carrier. To avoid the need of dynamic polarization control in front of the receiver, several methods have been proposed [9–11]. To get rid of precise optical filtering [9] and an extra frequency gap [10], the difference between the frequencies of two polarization-orthogonal reference carriers was set as one subcarrier spacing in [11]. Nonetheless, the frequency gap is still required, leading to lower SE and higher bandwidth requirement of a receiver.

This work simultaneously employs the PDM scheme [11] and removes the frequency gap to improve the SE of a DD-OFDM system. The resulting polarization-dependent interference in the gap-less DD-PDM-OFDM system is composed of linear inter-carrier interference (ICI) and nonlinear SSBI, which are caused by the PDM scheme and gap-less modulation, respectively. In order to remove the mixed polarization-dependent interference, we propose a novel iterative multiple-input multiple-output (MIMO) detection scheme. Compared to the detection scheme in [11], which only removes ICI, further eliminating the polarization-dependent SSBI using the proposed scheme can achieve the improvement of ~ 7 dB in signal-to-noise ratio (SNR) in the gap-less system. Employing the proposed scheme, we experimentally demonstrate a 39.5-Gbps DD-PDM-OFDM signal with 7-GHz bandwidth. Without dispersion-induced penalty and the need for polarization control, the 39.5-Gbps signal can achieve the FEC limit (i.e., bit-error rate (BER) of 10^{-3}) after transmission over single-mode fiber of 100 km.

#253910 Received 13 Nov 2015; revised 8 Jan 2016; accepted 12 Jan 2016; published 22 Jan 2016

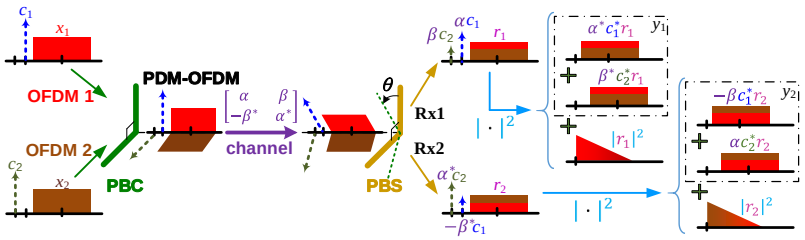

Fig. 1. The origin of linear and nonlinear interference (PBC: polarization beam combiner).

2. Principle of the proposed scheme

As shown in Fig. 1, two polarization-orthogonal OFDM signals, $x_1(t)$ and $x_2(t)$, are at the same frequency, but the frequency of a reference carrier, c_2, is shifted by one subcarrier spacing with respect to the other carrier, c_1. Thanks to the difference in the carrier frequencies, the fading of a carrier after a polarization-beam splitter (PBS) can be prevented without controlling received SoP. Omitting dispersion and loss for the sake of simplicity, the fiber channel could be treated as a frequency-irrelevant random orientated Jones matrix, which is unitary, and it follows,

$$\underbrace{\begin{bmatrix}\alpha & \beta\\ -\beta^* & \alpha^*\end{bmatrix}}_{\text{unitary: } |\alpha|^2+|\beta|^2=1}\left(\begin{bmatrix}0\\ c_2\end{bmatrix}+\begin{bmatrix}c_1\\ 0\end{bmatrix}+\begin{bmatrix}x_1\\ x_2\end{bmatrix}\right)=\underbrace{\begin{bmatrix}\alpha c_1+\beta c_2\\ -\beta^* c_1+\alpha^* c_2\end{bmatrix}}_{\text{carriers}}+\underbrace{\begin{bmatrix}\alpha x_1+\beta x_2\\ -\beta^* x_1+\alpha^* x_2\end{bmatrix}}_{\triangleq [r_1\ r_2]^{\mathrm{T}}}. \tag{1}$$

It should be noted that $\theta \triangleq \tan^{-1}|\beta/\alpha|$ is relevant to the performance of the PDM scheme [11]. For the upper receiver in Fig. 1 and (1), the signal after square-law detection becomes,

$$\underbrace{|\alpha c_1+\beta c_2|^2}_{\text{carrier-to-carrier}}+\underbrace{r_1(\beta c_2+\alpha c_1)^*}_{\text{linear signal}\triangleq y_1}+\underbrace{r_1^*(\beta c_2+\alpha c_1)}_{=y_1^*}+\underbrace{|r_1|^2}_{\text{SSBI}}, \tag{2}$$

where the first term can be omitted in the following discussion due to its low frequency. The detected linear signal y_1 contains linear interference caused by not only signal mixing at the same frequency (i.e., $r_1=\alpha x_1+\beta x_2$) but also the ICI due to the different frequencies of carriers (e.g., the combination of $c_1^* x_1$ and $c_2^* x_1$). The linear signal y_2 at the lower receiver has the similar situation. Thus, using $X_{k,i}/Y_{k,i}$ to denote the ith discrete frequency components (i.e., the ith subcarriers) of time-domain signals x_k/y_k, the MIMO channel is as follow (i.e., (3) in [11]),

$$\begin{bmatrix}Y_{1,i}\\ Y_{2,i}\end{bmatrix}=\begin{bmatrix}\alpha\beta^* & |\beta|^2 & |\alpha|^2 & \alpha^*\beta\\ -\alpha\beta^* & |\alpha|^2 & |\beta|^2 & -\alpha^*\beta\end{bmatrix}\begin{bmatrix}X_{1,i-1}\\ X_{2,i-1}\\ X_{1,i}\\ X_{2,i}\end{bmatrix}\triangleq\underbrace{\begin{bmatrix}h_{11} & h_{12} & h_{13} & h_{14}\\ h_{21} & h_{22} & h_{23} & h_{24}\end{bmatrix}}_{\text{MIMO matrix: }\mathbf{H}_i}\begin{bmatrix}X_{1,i-1}\\ X_{2,i-1}\\ X_{1,i}\\ X_{2,i}\end{bmatrix}. \tag{3}$$

Furthermore, to further increase the SE by removing the frequency gap, the detected linear signals are interfered by the nonlinear SSBI in the form of,

$$\begin{aligned}|r_1|^2&=\left|\alpha\left(x_1+\frac{\beta}{\alpha}x_2\right)\right|^2=|\alpha|^2\times\left|x_1+x_2e^{-j(\phi_\alpha-\phi_\beta)}\tan\theta\right|^2,\\ |r_2|^2&=\left|-\alpha^*\left(\frac{\beta^*}{\alpha^*}x_1-x_2\right)\right|^2=|\alpha|^2\times\left|x_1e^{j(\phi_\alpha-\phi_\beta)}\tan\theta-x_2\right|^2,\end{aligned} \tag{4}$$

where $\alpha\triangleq|\alpha|e^{j\phi_\alpha}$ and $\beta\triangleq|\beta|e^{j\phi_\beta}$. If x_1 and x_2 are known, only the amplitude ratio $|\alpha/\beta|$ and phase difference $\Delta\phi=\phi_\alpha-\phi_\beta$ are required for estimating SSBI, in accordance with (4). Therefore, to remove the linear and nonlinear interference, the proposed procedure is as follows,

#253910 Received 13 Nov 2015; revised 8 Jan 2016; accepted 12 Jan 2016; published 22 Jan 2016

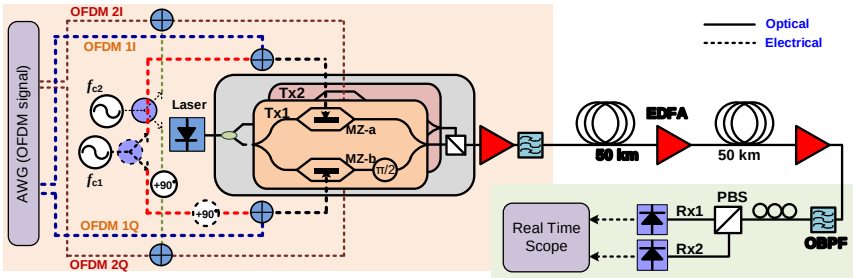

Fig. 2. Experiment setup (OBPF: optical bandpass filter).

1. Using training symbols to estimate the MIMO matrices $\mathbf{H}_i$ and to extract $|\alpha/\beta|$ and $\Delta\phi$ from $\mathbf{H}_i$.
   The MIMO matrices could be characterized by time- and frequency-multiplexed training symbols, as detailed in [12]. Then, in accordance with (3), $|\alpha/\beta|$ and $\Delta\phi$ can be estimated from h_{12}/h_{22} (or h_{13}/h_{23}) and h_{11}/h_{14} (or h_{21}/h_{24}), respectively.
2. Estimating x_1 and x_2 via the PDM-MIMO detection, which eliminates the linear interference.
   As detailed in [11], utilizing the pseudo-inverse of the non-square channel matrices can estimate the sent data $X_{1,i}$ and $X_{2,i}$ in the presence of SSBI.
3. Calculating the SSBI based on the knowledge obtained in step 1 and 2 to remove the SSBI from the detected signals.
   Because x_1 and x_2 are estimated in the form of frequency components $X_{1,i}$ and $X_{2,i}$ in step 2, inverse fast Fourier transform (IFFT) is needed before calculating the SSBI via (4). The obtained time-domain SSBI (i.e., $|r_1|^2$ and $|r_2|^2$) will be transferred back to the frequency domain using fast Fourier transform (FFT) before conducting SSBI cancellation.
4. Repeating step 2 and 3 iteratively to decrease the decision errors in step 2 and to improve the accuracy of estimating the SSBI in step 3.
   It should be noted that the estimation of $X_{1,i}$ and $X_{2,i}$ in step 2 is based on the received signals with the removal of the latest updated SSBI.

The computational complexity required for SSBI cancellation is mainly contributed by additional IFFT and FFT described in step 3. Thus, the SSBI cancellation requires $\mathcal{O}(N\log_2 N)$ operations for each iteration, where N denotes the FFT size.

3. Experiment setup and results

Figure 2 shows the experiment setup. By electrically combining baseband OFDM signals and sinusoidal waves, two polarization-orthogonal DD-OFDM signals were generated by a dual-polarization optical IQ modulator. The frequencies of the sinusoidal waves, which generated the optical reference carriers, were 3.5156 and 3.5390 GHz such that the difference equals the subcarrier spacing. Two sets of the electrical IQ OFDM signals were generated by an arbitrary waveform generator (Agilent® AWG M8190) with 4 independent digital-to-analog conversion (DAC) channels. The sampling rate and DAC resolution of the AWG were 12 GS/s and 12 bits, respectively. The OFDM signal contained 294 subcarriers with the Fast-Fourier transform size of 512 and the cyclic prefix of 1/16. The bandwidth of the OFDM signal was 7 GHz, yielding that the frequency gap was almost 0. For comparison, the gap is required to $\geq$7 GHz in traditional DD-OFDM systems; thus, the bandwidth requirement of the receiver was lowered by 7 GHz in our system. To reduce the condition number (CN) of the MIMO channel, an empty tone was inserted every 6 subcarriers [11,12]. After single-mode fiber transmission of 100 km, a

#253910 Received 13 Nov 2015; revised 8 Jan 2016; accepted 12 Jan 2016; published 22 Jan 2016

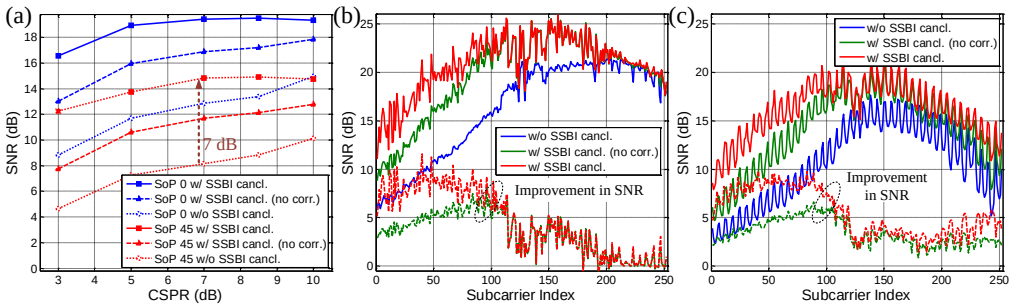

Fig. 3. (a) Average SNRs of all subcarriers as functions of CSPR. At the CSPR of 7 dB, the average SNR of each subcarrier with the SoP of (b) 0 and (c) 45°.

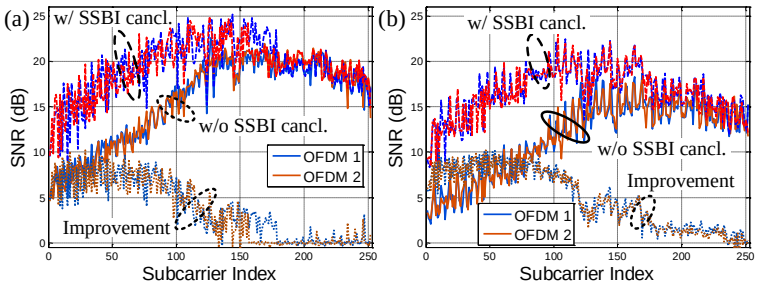

Fig. 4. Measured SNR of the bit-loaded signal with SoP of (a) 0 and (b) 45°.

polarization controller (PC) was inserted in front of the polarization-diverse receiver to control the received SoP, such that the signal performance can be evaluated over different conditions; i.e., different θ. After the PBS and photo-detectors (XPDV3120R), the signals were captured by a digital oscilloscope (Agilent® DSOX 91604A) with 40-GS/s sampling rate. The off-line DSP program was used to carry out the proposed MIMO detection.

For DD-OFDM systems, the carrier-to-signal power ratio (CSPR) is a critical parameter. Figure 3(a) shows the measured average SNR versus different CSPR using a fixed format of 16 QAM and the received optical power of 1 dBm. Two extreme cases of the received SoP are under discussion: $\theta = 0$ and 45° [11]. The former indicates the ideal case without polarization mixing and $|\alpha| = 1$, and the other one indicates the worse case, in which two polarization-orthogonal signals are equally mixed in each detector and $|\alpha| = |\beta|$. The cases without SSBI cancellation in the following discussion represents the MIMO detection is applied without the mitigation of the nonlinear interference. In Fig. 3, the improvement in SNR with SoP of 0 can be $\sim$ 8 dB using low CSPR, and it slightly decreases as increasing CSPR. Similar trend can be observed in the case with SoP of 45°. It should be noted that decision errors made in the PDM-MIMO detection is omitted in estimating SSBI in Fig. 3. Because the worse case would dominate the system performance, we select the CSPR of 7 dB, which is roughly the optimal value for the case with SoP of 45°, in the following experimental investigation. Based on the CSPR of 7 dB, Figs. 3(b) and 3(c) show the average SNR of each subcarrier with and without SSBI cancellation under the SoP of 0 and 45°, respectively. The improvement in SNR at lower frequencies is more than that at higher frequencies because more SSBI is created at lower frequencies, as depicted in Fig. 1. Moreover, because the transmitter, particularly the AWG, has limited frequency response, we must use the measured response to adjust the related amplitudes of data, which were estimated in step 2 of the proposed procedure. Figure 3 also

#253910 Received 13 Nov 2015; revised 8 Jan 2016; accepted 12 Jan 2016; published 22 Jan 2016

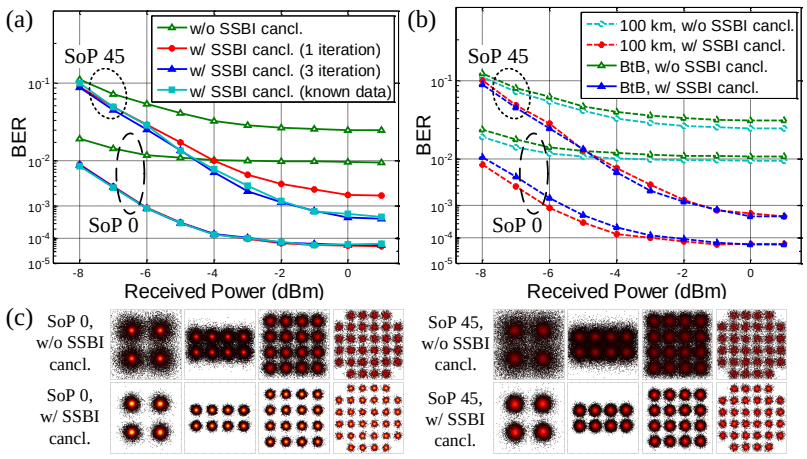

Fig. 5. (a) BER curves at BtB with different SSBI cancellation, (b) BER curves at BtB and after 100-km fiber, and (c) selected constelations.

shows the results of the proposed MIMO detection without the correction (denoted by "no corr." in the legend), which indicates the calculation of SSBI neglects the limited response of the transmitter, and the difference in SNR reveals the necessity of correcting the frequency response in calculating SSBI. Without the correction, the improvement in SNR is lowered by ~ 3 dB at the CSPR of 7 dB in Fig. 3(a). In accordance with the SNR of the 16-QAM OFDM signal with SoP of 45° at the received power of 1 dBm, we applied the bit-loading scheme [13] to allocate the best combination of powers and modulation formats of subcarriers, resulting in the maximum capacity of 39.5 Gbps. Figures 4(a) and 4(b) plot the SNR of each bit-loaded subcarrier of two independent OFDM signals with the SoP of 0 and 45°, respectively. Because decision errors in the PDM-MIMO detection was taken into consideration for the bit-loaded signals, iteration of SSBI cancellation is required and was set 3 times. Figure 5(a) plots the BER curves of the bit-loaded signal at optical back-to-back (BtB) using the proposed scheme with different iteration times. The results without considering decision errors (i.e., using known data) are also shown to be the upper bounds of the performance. The BER with the proposed scheme of 3 iterations can perform as good as the upper bounds, revealing that 3 iterations are sufficient. Besides, the signal cannot reach the BER of 10^{-3} until applying the proposed detection. Figure 5(b) compares the BER results at optical BtB and after 100-km fiber, and the fact that the BER curves at BtB and after transmission coincide indicates that the signal and the proposed detection scheme are dispersion-tolerant. The sensitivity difference between the cases with the SoP of 0 and 45° is around 4 dB, which is caused by different CN of the channel, and the difference can be reduced by employing nonlinear detection [14]. Figure 5(c) shows selected constellations after transmission to demonstrate the effectiveness of the proposed scheme.

4. Conclusion

This work experimentally demonstrates a gap-less DD-PDM-OFDM sytem to seek for higher SE and to lower bandwidth requirement of components. In such a system, we propose the novel MIMO detection scheme to eliminate the polarization-dependent linear and nonlinear interference, and the scheme achieved the improvement of 7 dB in SNR by eliminating polarization-dependent SSBI. A 39.5-Gbps DD-PDM-OFDM signal was generated within 7-GHz bandwidth in the proposed system, and the signal was transmitted over single-mode fiber of 100 km without dispersion-induced penalty and the need for polarization control.

#253910 Received 13 Nov 2015; revised 8 Jan 2016; accepted 12 Jan 2016; published 22 Jan 2016